Running Title: PolyQ tract length and huntingtin aggregation

SUPPLEMENTARY MATERIAL

Subcellular localisation and formation of huntingtin aggregates correlates with symptom onset and progression in a Huntington's disease model

Christian Landles[1], Rebecca E. Milton[1], Nadira Ali[1], Rachel Flomen[1], Michael Flower[1], Franziska Schindler[2], Casandra Gomez-Paredes[1], Marie K. Bondulich[1], Georgina F. Osborne[1], Daniel Goodwin[1], Grace Salsbury[1], Caroline L. Benn[1,3], Kirupa Sathasivam[1], Edward J. Smith[1], Sarah J. Tabrizi[1], Erich E. Wanker[2] and Gillian P. Bates[1]

[1]Huntington's Disease Centre, Department of Neurodegenerative Disease and UK Dementia Research Institute at UCL, Queen Square Institute of Neurology, UCL, Queen Square, WC1N 3BG, UK.
[2]Neuroproteomics, Max Delbrueck Center for Molecular Medicine, 13125 Berlin, Germany and Berlin Institute of Health (BIH), 10178 Berlin, Germany.
[3]LoQus23 Therapeutics, Babraham Research Campus, Cambridge, CB22 3AT, UK.

Correspondence to: Gillian Bates (PhD)
Huntington's Disease Centre, Department of Neurodegenerative Disease and UK Dementia Research Institute at UCL
Queen Square Institute of Neurology, UCL
Queen Square
LondonWC1N 3BG, UK
Email: gillian.bates@ucl.ac.uk

Supplementary Figure 1

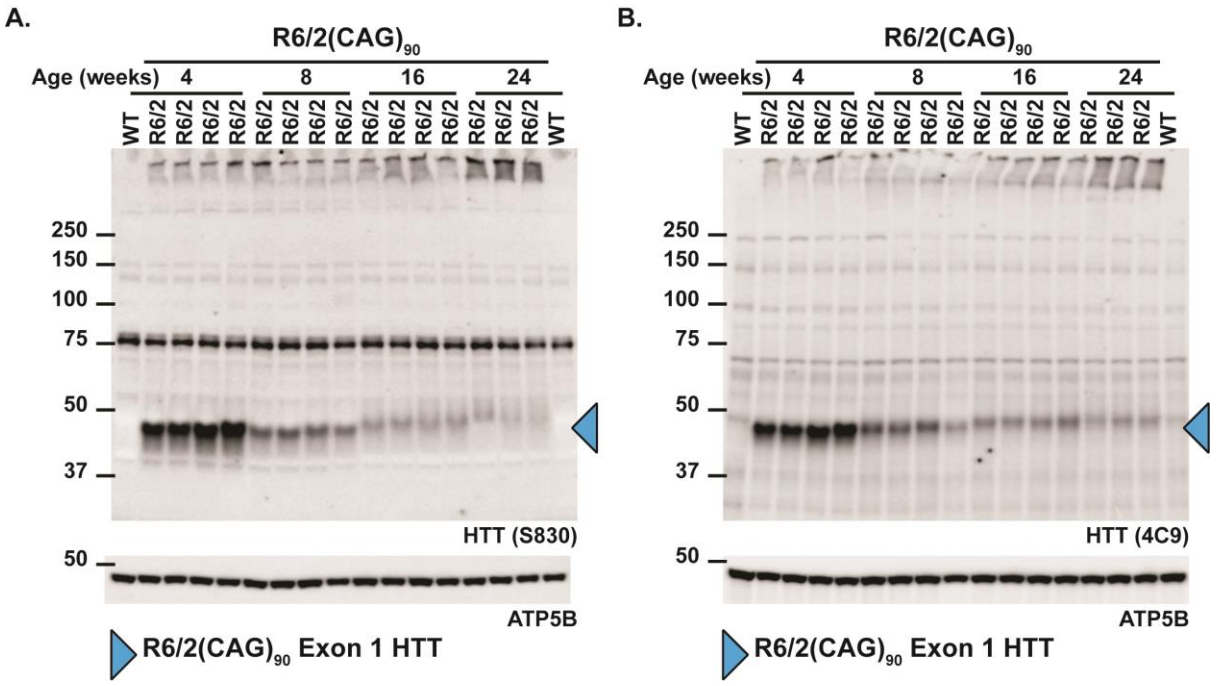

Supplementary Figure 1. The migration of the exon 1 HTT protein becomes increasingly retarded with age in the R6/2(CAG)$_{90}$ mice.

Western blot analysis of soluble and aggregated exon 1 HTT protein in brain lysates from R6/2(CAG)$_{90}$ mice at 4, 8, 16 and 24 weeks of age immunoprobed with (**A**) S830 or (**B**) 4C9 antibodies. ATP5B was used as a loading control. Aggregated HTT was already prominent in the stacking gel for R6/2(CAG)$_{90}$ mice at 4 weeks of age. The migration of soluble exon1 HTT became increasingly retarded with age, possibly reflecting somatic instability of the CAG repeat. The full-sized loading control blots are shown in Supplementary Fig. 12. WT = wild type.

Supplementary Figure 2

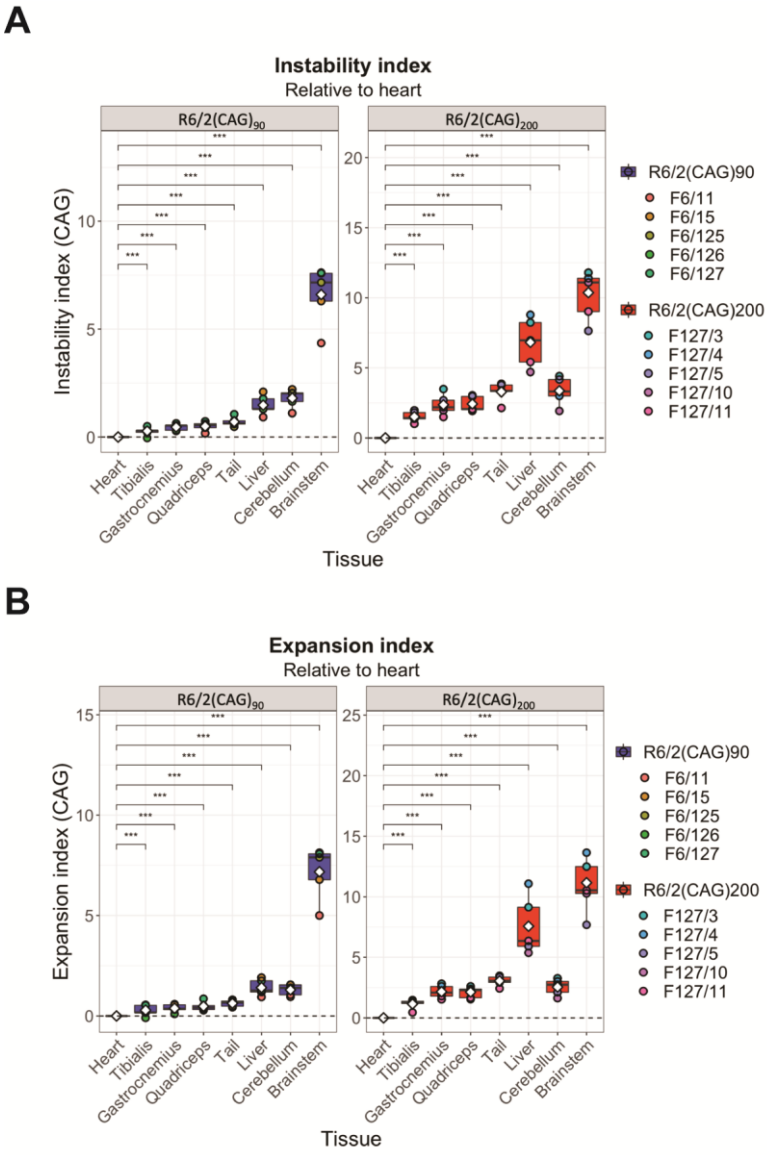

Supplementary Figure 2. Instability and expansion indices for the extent of somatic instability in the R6/2(CAG)$_{90}$ and R6/2(CAG)$_{200}$ mice. The mean, standard deviation and data points for the (**A**) instability and (**B**) expansion indices of each tissue are illustrated.

Supplementary Figure 3

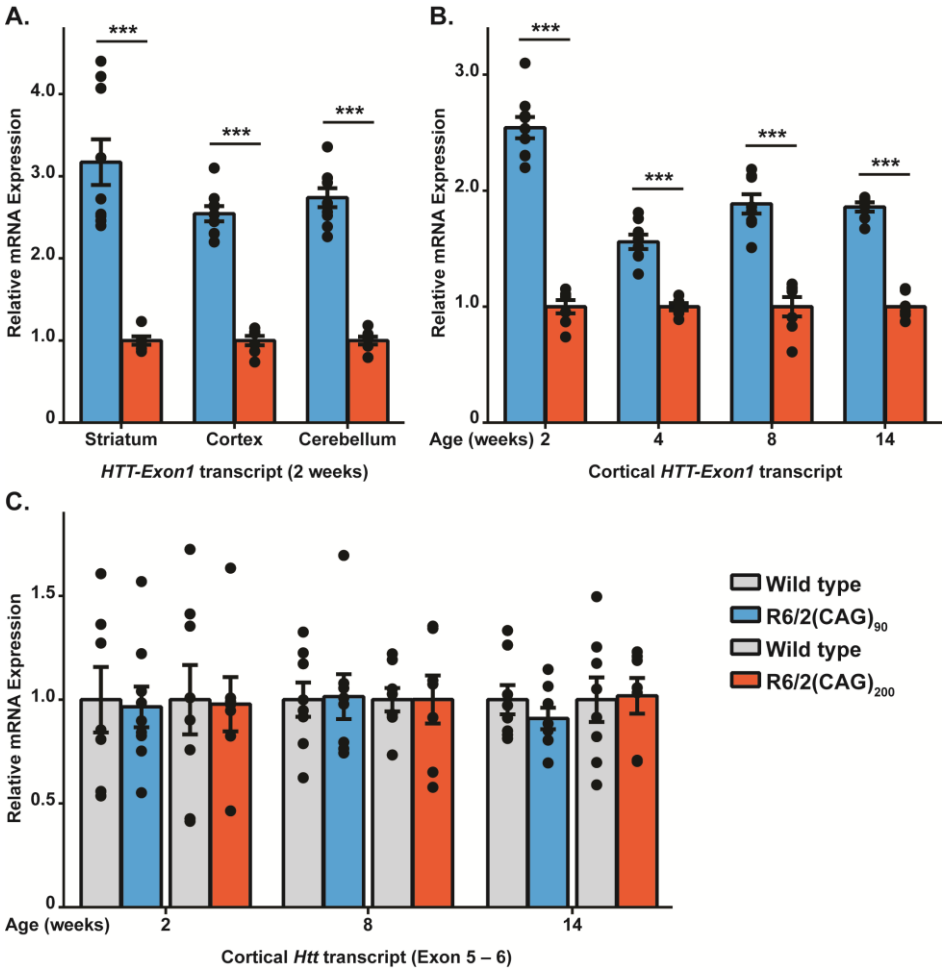

Supplementary Figure 3. The R6/2 transcript was expressed at higher levels in R6/2(CAG)$_{90}$ as compared to R6/2(CAG)$_{200}$ brain regions.

(**A**) Comparative levels of the *HTT* exon 1 transgene mRNA as measured by qPCR in brain regions from R6/2(CAG)$_{90}$ and R6/2(CAG)$_{200}$ mice at 2 weeks of age. R6/2(CAG)$_{90}$ levels were 2.5 – 3 fold higher in R6/2(CAG)$_{90}$ than in R6/2(CAG)$_{200}$ brain regions. (**B**) Comparative levels of the *HTT* exon 1 transgene mRNA as measured by qPCR in the cortex of R6/2(CAG)$_{90}$ and R6/2(CAG)$_{200}$ mice at 2, 4, 8 and 14 weeks of age. R6/2(CAG)$_{90}$ transcript levels remained approximately 2 fold higher in R6/2(CAG)$_{90}$ than in R6/2(CAG)$_{200}$ mice from 4 to 14 weeks of age. (**C**) The levels of endogenous *Htt* were comparable in the cortex of R6/2(CAG)$_{90}$, R6/2(CAG)$_{200}$ and their wild type littermates at 2, 8 and 14 weeks of age. (**A, C**) R6/2(CAG)$_{90}$ (n = 9), R6/2(CAG)$_{200}$ (n = 7), wild type (CAG)$_{90}$ (n = 7), wild type (CAG)$_{200}$ (n = 8). (**B**) n = 8 / genotype. Statistical analysis was two-tailed Student's *t*-test or two-way ANOVA with Bonferroni *post hoc* correction. The test statistic, degrees of freedom and *p* values for the ANOVA are provided in Supplementary Table 8. ***p ≤ 0.001.

Supplementary Figure 4

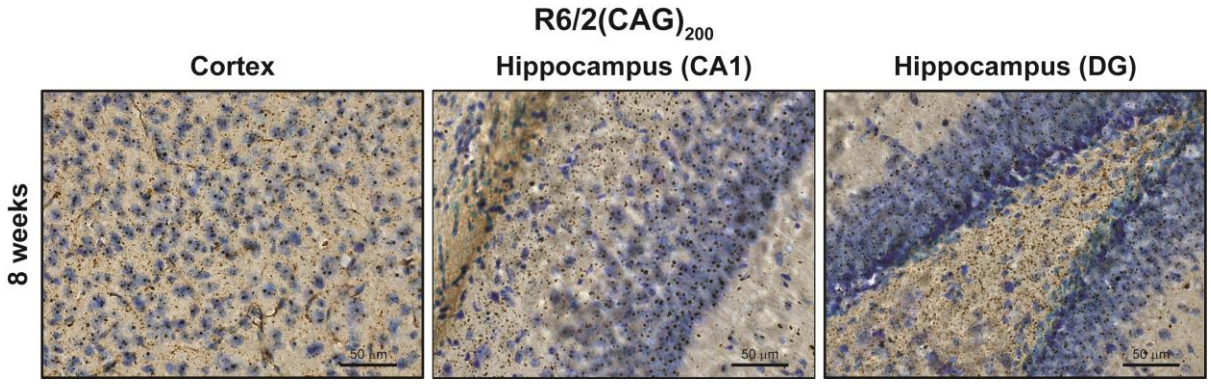

Supplementary Figure 4. Brain sections from R6/2(CAG)$_{200}$ mice immunoprobed with MW8 and counterstained with thionin to show the location of nuclei.

Sections from the cortex, the CA1 region of the hippocampus and dentate gyrus from R6/2(CAG)$_{200}$ mice at 8 weeks of age immunoprobed with MW8 and counterstained with thionin. At this age, nuclear aggregation in the R6/2(CAG)$_{200}$ mice appeared as an inclusion, whereas in the R6/2(CAG)$_{90}$ mice, aggregated HTT appeared as a diffuse signal that filled the entire nucleus (Fig. 5) DG = dentate gyrus. n = 3 / R6/2 genotype and n = 1 / wild type control. Scale bar = 50 µm.

Supplementary Figure 5

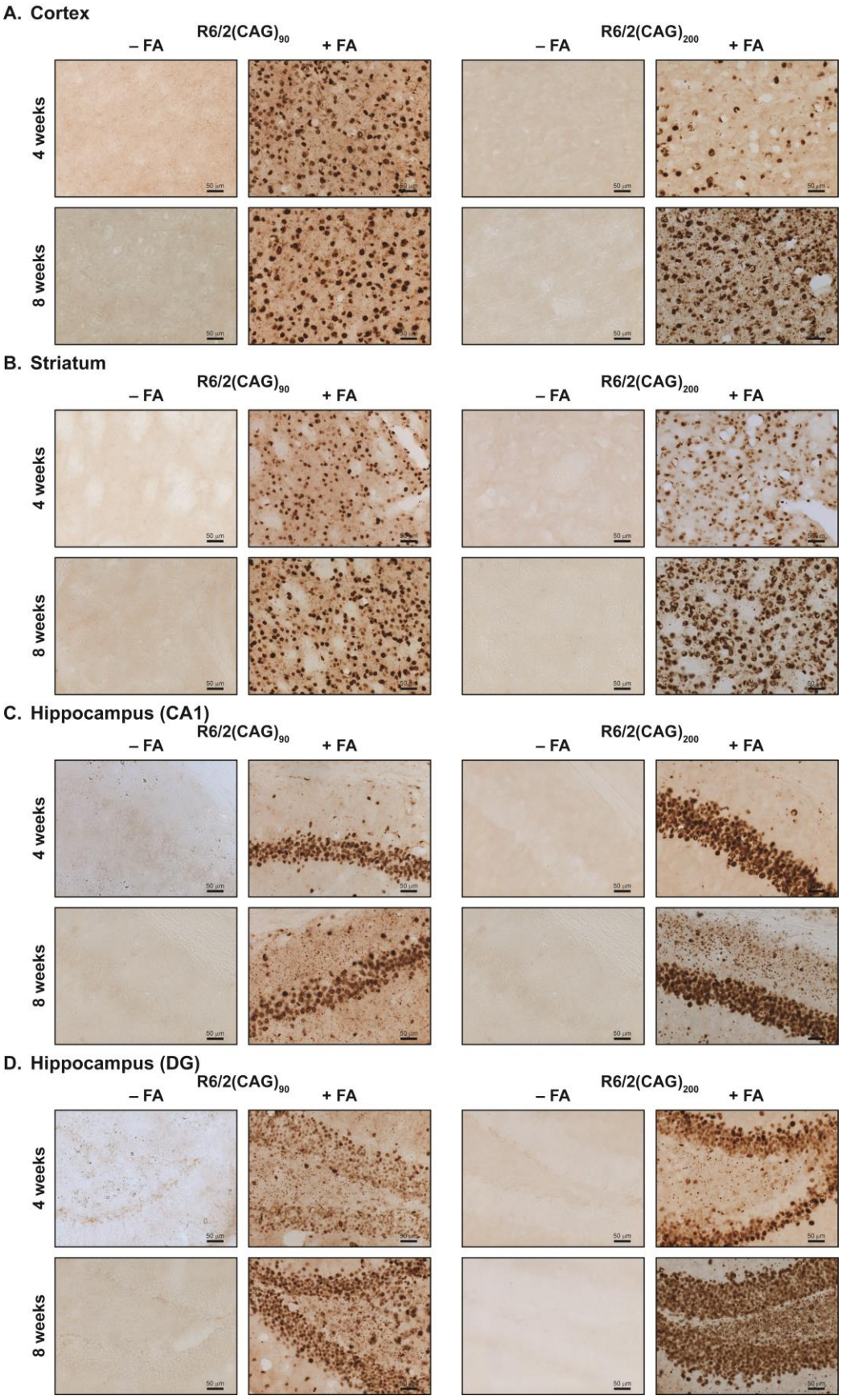

Supplementary Figure 5. Antigen retrieval with formic acid revealed the presence of aggregated HTT in brain sections from R6/2(CAG)$_{90}$ and R6/2(CAG)$_{200}$ mice.

Sections from the (**A**) cortex, (**B**) striatum, (**C**) CA1 region of the hippocampus and (**D**) dentate gyrus of the hippocampus from R6/2(CAG)$_{90}$ and R6/2(CAG)$_{200}$ mice at 4 and 8 weeks of age were immunoprobed with the 4H7H7 antibody that detects polyglutamine peptides. No signal was obtained (-FA). Pre-treatment with formic acid (+FA) exposed the polyglutamine epitopes within huntingtin aggregates, allowing detection with 4H7H7, and demonstrating that the diffuse staining pattern detected with the MW8 antibody in Figs. 5 and 6 represented an aggregated form of HTT. The extent of cytoplasmic aggregation was greater in the R6/2(CAG)$_{200}$ hippocampus at 8 weeks of age than the R6/2(CAG)$_{90}$ hippocampus, both (**C**) dorsal to the CA1 and (**D**) in the hilus (cleft of the dentate gyrus). FA = formic acid. DG = dentate gyrus. n = 3 / R6/2 genotype and n = 1 / wild type control. Scale bar = 50 µm.

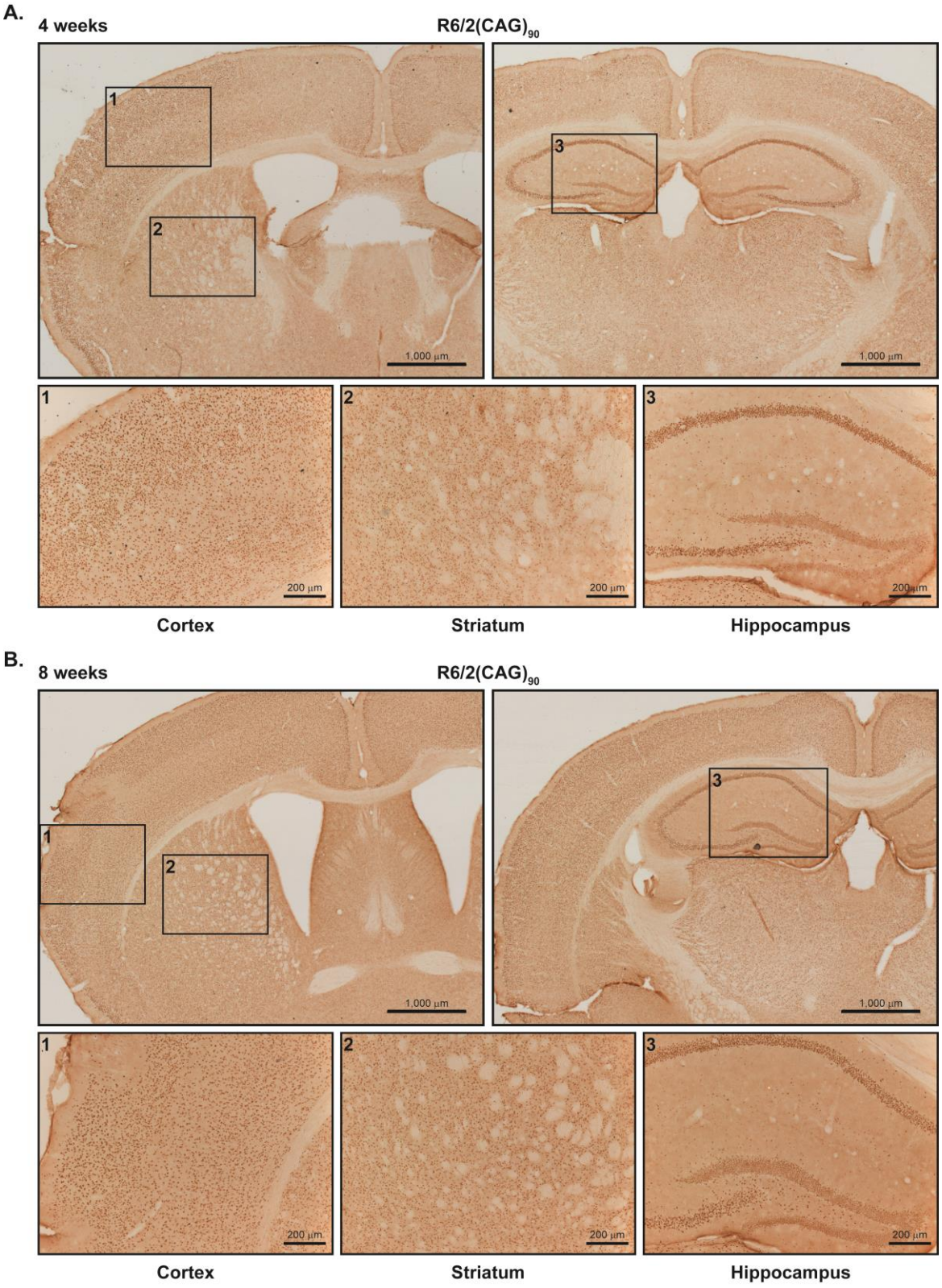

Supplementary Figure 6. Huntingtin aggregation in R6/2(CAG)$_{90}$ brains.
The pattern of HTT aggregation in coronal sections from R6/2(CAG)$_{90}$ brains immunoprobed with MW8 at (**A**) 4 and (**B**) 8 weeks of age. The three boxes below the main panels indicate the location of the images shown in Figs. 5 and 6A. n = 3 / R6/2 genotype and n = 1 / wild type control. Scale bar = 1,000 µm (upper), 200 µm (lower).

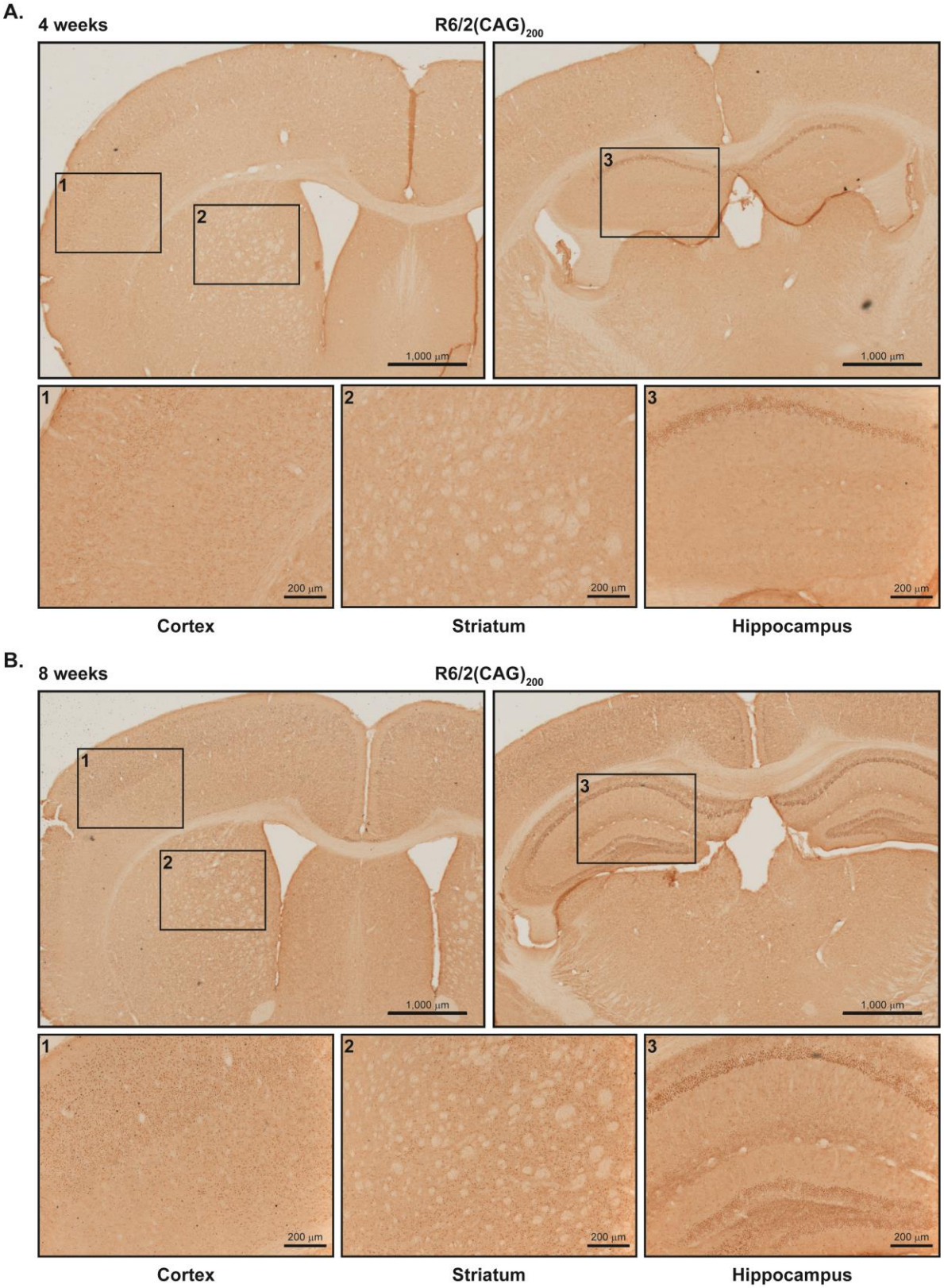

Supplementary Figure 7. Huntingtin aggregation in R6/2(CAG)$_{200}$ brains.
The pattern of HTT aggregation in coronal sections from R6/2(CAG)$_{200}$ brains immunoprobed with MW8 at (**A**) 4 and (**B**) 8 weeks of age. The three boxes below the main panels indicate the location of the images shown in Figs. 5 and 6A. n = 3 / R6/2 genotype and n = 1 / wild type control. Scale bar = 1,000 µm (upper), 200 µm (lower).

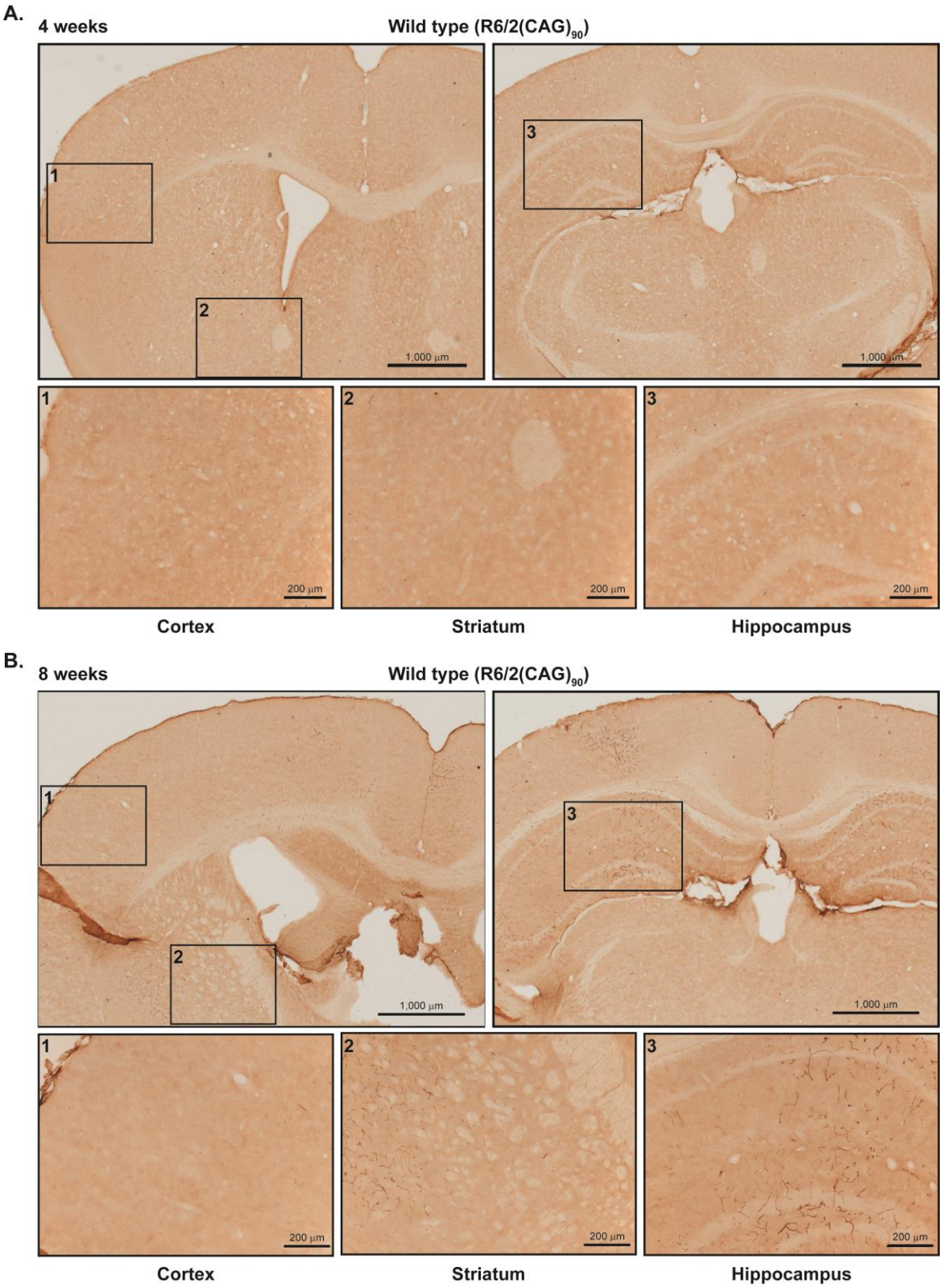

Supplementary Figure 8. Wild Type controls for sections immunoprobed with MW8.
Coronal sections from wild type controls for the R6/2(CAG)$_{90}$ brains immunoprobed with MW8 at (**A**) 4 and (**B**) 8 weeks of age, shown in Supplementary Fig. 6. n = 3 / R6/2 genotype and n = 1 / wild type control. Scale bar = 1,000 µm (upper), 200 µm (lower).

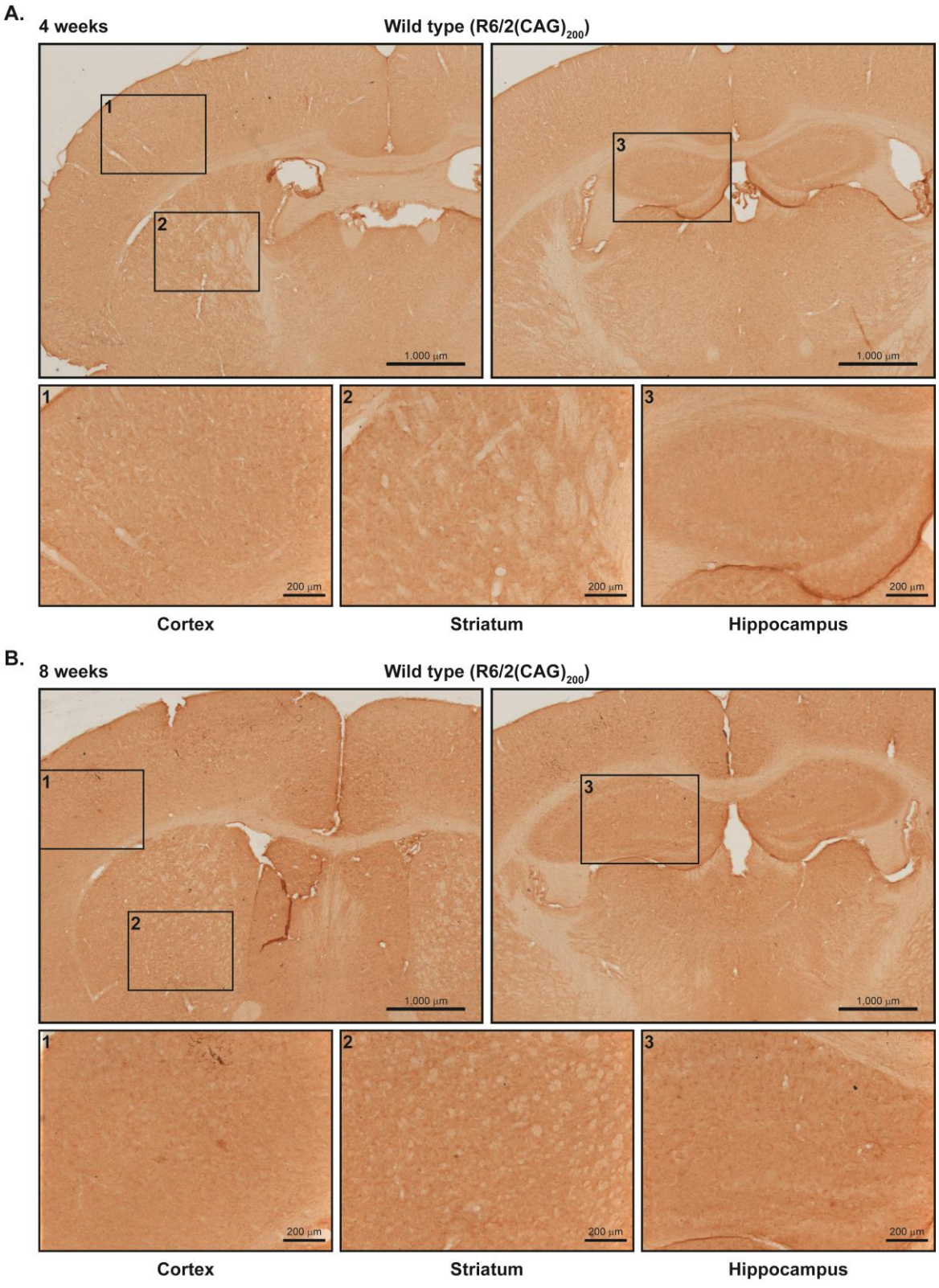

Supplementary Figure 9. Wild Type controls for sections immunoprobed with MW8.
Coronal sections from wild type controls for the R6/2(CAG)$_{200}$ brains immunoprobed with MW8 at (**A**) 4 and (**B**) 8 weeks of age, shown in Supplementary Fig. 7. n = 3 / R6/2 genotype and n = 1 / wild type control. Scale bar = 1,000 µm (upper), 200 µm (lower).

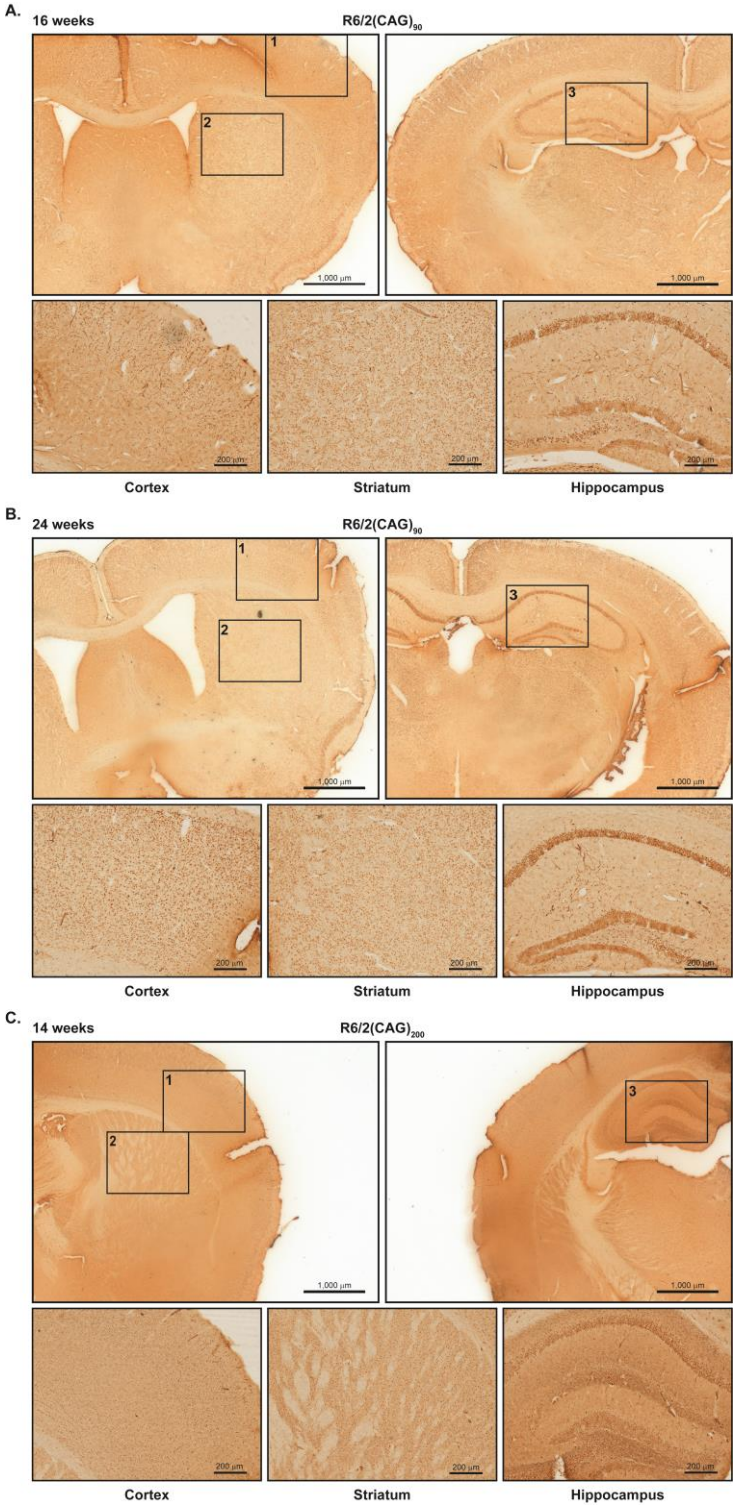

Supplementary Figure 10. Huntingtin aggregation in R6/2(CAG)$_{90}$ and R6/2(CAG)$_{200}$ brains. The pattern of HTT aggregation in coronal sections from R6/2(CAG)$_{90}$ at (**A**) 16 and (**B**) 24 weeks of age and (**C**) R6/2(CAG)$_{200}$ at 14 weeks of age immunoprobed with MW8. The three boxes below the main panels indicate the location of the images shown in Fig. 6B. n = 3 / R6/2 genotype and n = 1 / wild type control. Scale bar = 1,000 µm (upper), 200 µm (lower).

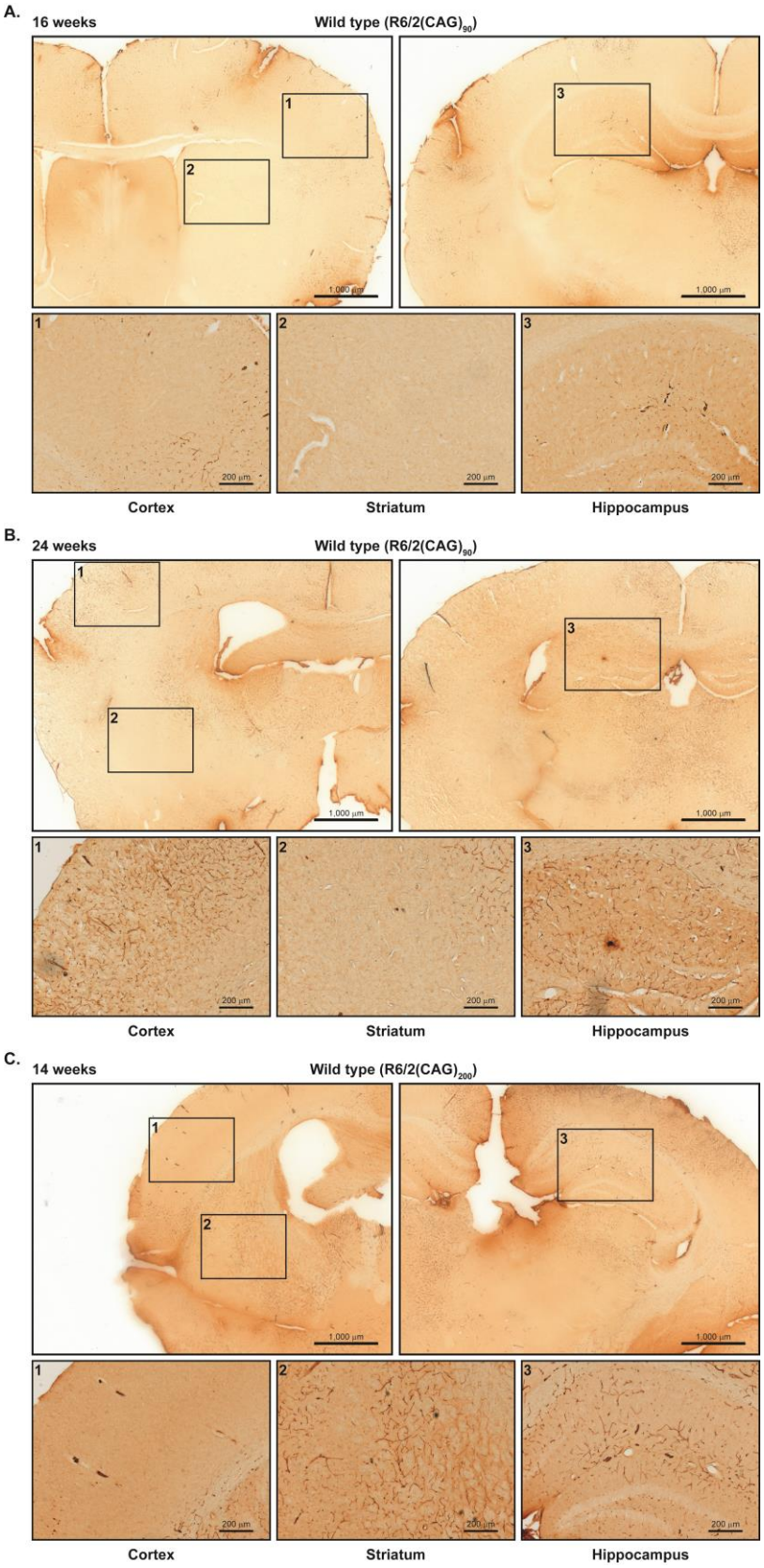

Supplementary Figure 11. Wild Type controls for sections immunoprobed with MW8.
Coronal sections from wild type controls for the R6/2(CAG)$_{90}$ at (**A**) 16 and (**B**) 24 weeks of age and (**C**) R6/2(CAG)$_{200}$ at 14 weeks immunoprobed with MW8 and shown in Supplementary Fig. 10. n = 3 / R6/2 genotype and n = 1 / wild type control. Scale bar = 1,000 µm (upper), 200 µm (lower).

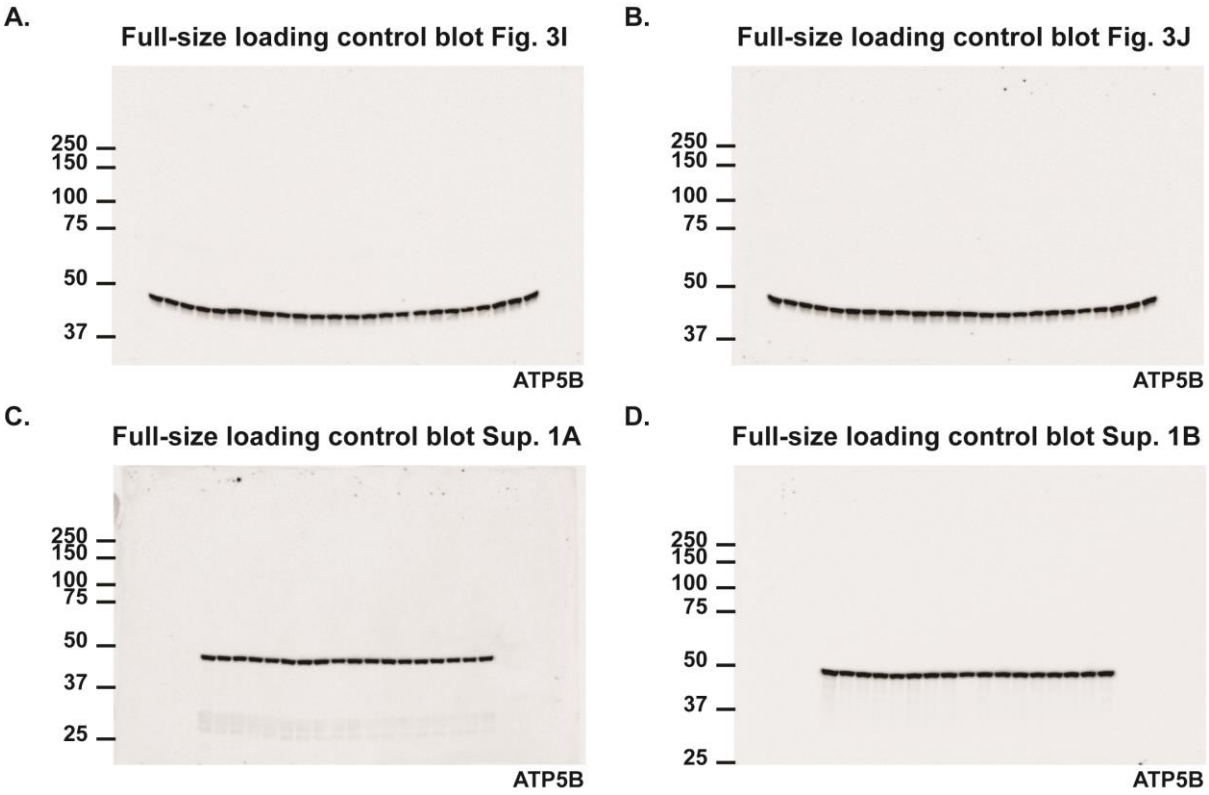

Supplementary Figure 12. Full-sized loading control blots.

Full-sized loading control blots immunoprobed with ATP5B for the western blots presented in (**A**) Fig. 3I, (**B**) Fig. 3J, (**C**) Supplementary Fig. 1A and (**D**) Supplementary Fig. 1B.

Supplementary Table 1. Real-time quantitative PCR assays

Gene	Supplier	Primer/Probe	Sequence (5' to 3') or Catalogue number
Atp5b	Primer Design		HK-DD-mo-900
Bdnf IV	Eurofins Genomics	Forward	CTGCCTTGATGTTTACTTTGACAAG
		Reverse	GCAACCGAAGTATGAAATAACCATAG
		Probe	TTCCACCAGGTGAGAAGAGTGATGACCAT
Canx	Primer Design		HK-DD-mo-900
Cnr1	Eurofins Genomics	Forward	CACAAGCACGCCAATAACACA
		Reverse	ACAGTGCTCTTGATGCAGCTTTC
		Probe	CAGCATGCACAGGGCCGC
Darpp32	Eurofins Genomics	Forward	CCCGACAGGTGGAGATGATC
		Reverse	GCTGCACAGCTTTCAGTGATG
		Probe	CTGCCATGCTTTTCCGGGTCTCAG
Drd2	Eurofins Genomics	Forward	ACACCACTCAAGGGCAACTGT
		Reverse	GGCGGGCAGCATCCA
		Probe	GGGTCAGGACATGAAACTCTGCACCG
Eif4a2	Primer Design		HK-DD-mo-900
Grm2	Thermo Fisher		Mm01235831_m1
Hrh3	Thermo Fisher		Mm00446706_m1
Htr1a	Thermo Fisher		Mm00434106_s1
HTT transgene	Eurofins Genomics	Forward	GCTGCACCGACCGTGAGT
		Reverse	CGCAGGCTGCAGGGTTAC
		Probe	CAGCTCCCTGTCCCGGCGG
Mouse Htt	Eurofins Genomics	Forward	CTCAGAAGTGCAGGCCTTACCT
		Reverse	GATTCCTCCGGTCTTTTGCTT
		Probe	TGAATCTTCTTCCATGCCTGACCCGA
Igfbp5	Eurofins Genomics	Forward	AAGGATTCTACAAGAGAAAGCAGTGTAA
		Reverse	ACTTGTCCACACACCAGCAGAT
		Probe	TCCCGTGGCCGCAAACGTG
Kcnk2	Eurofins Genomics	Forward	GACTACGTGGCAGGTGGATCA
		Reverse	GCCAGCCCAACGAGGAT
		Probe	AATATCTGGACTTCTACAAGCCTGTGGTGTG
Nr4a2	Eurofins Genomics	Forward	ATTTCCTCGAAAACTCCAATAACTCT
		Reverse	TGAGGCGAGGACCCATACTG
		Probe	CTGAAGCCATGCCTTGTGTTCAGGC
Pcp4	Eurofins Genomics	Forward	CTGAGCTGTTCTGTGGGACCTA
		Reverse	CGCTCCGGCACTTTGTCT
		Probe	CTGCGGAGTCAGGCCAACATGA
Pde10a	Primer Design	Forward	TTGGCAAGTGGAGCATATTTAAC
		Reverse	CCTGGAAACCTTTGGAGAGAAA
		Probe	Custom assay / not supplied
Penk1	Eurofins Genomics	Forward	ATGCAGCTACCGCCTGGTT
		Reverse	GCAGCTGTCCTTCACATTCCA
		Probe	AGGCGACATCAATTTCCTGGCGTG
Pgam2	Primer Design	Forward	GGGAGGAGCAGGTGAAGAT
		Reverse	GATGGAGGTGTAGTAGTTGTGTT
		Probe	Custom assay / not supplied
Rpl13a	Primer Design		HK-DD-mo-900
Uchl1	Eurofins Genomics	Forward	GGTACCATCGGGTTGATCCA
		Reverse	AACTGTTTCAGGACGGATCCA
		Probe	AACCAAGACAAGCTGGAATTTGAGGA
Ubc	Primer Design		HK-DD-mo-900

Supplementary Table 2. Summary of antibodies

Name	Immunogen	Epitope	Species	Concentration	Reference / Source
S830	HTT exon1 (53Q)		Sheep polyclonal	WB (1:2,000)	(Sathasivam *et al.*, 2001) in-house
Biotinylated 4H7H7	HTT N171 (65Q)	PolyQ	Mouse monoclonal	IHC (1:3,000)	(Landles *et al.*, 2010) Alex Osmand
4C9	HTT peptide: aa 51-71		Mouse monoclonal	WB (1:1,000) ELISA (1:1,000)	(Landles *et al.*, 2010) CHDI Foundation
MAB5374 (EM48)	HTT N256 (0Q)	Exon 1 HTT*	Mouse monoclonal	WB (1:500)	(Wang *et al.*, 2008) Millipore MAB5374
MW8	HTT exon1 (67Q)	aa 83-90	Mouse monoclonal	WB (1:1,000) IHC (1:2,000) ELISA (1:2,000)	(Ko *et al.*, 2001) CHDI Foundation
ATP5B	Human heart mitochondria		Mouse monoclonal	WB (0.5 µg/ml)	Abcam, ab14730
α-tubulin	Chick brain tubulin		Mouse monoclonal	WB (1:40,000)	Sigma, T9026
Histone-H3	Human synthetic peptide		Rabbit polyclonal	WB (1:50,000)	Millipore, 07-690

aa = amino acid; WB = western blot; IHC = immunohistochemistry

*EM48 detects an epitope in the C-terminal region of human exon 1 HTT and requires the VA dipeptide present in human HTT but absent from the mouse protein.

REFERENCES

Ko J, Ou S, Patterson PH. New anti-huntingtin monoclonal antibodies: implications for huntingtin conformation and its binding proteins. Brain Res Bull 2001; 56(3-4): 319-29.

Landles C, Sathasivam K, Weiss A, Woodman B, Moffitt H, Finkbeiner S*, et al.* Proteolysis of mutant huntingtin produces an exon 1 fragment that accumulates as an aggregated protein in neuronal nuclei in Huntington disease. J Biol Chem 2010; 285(12): 8808-23.

Sathasivam K, Woodman B, Mahal A, Bertaux F, Wanker EE, Shima DT*, et al.* Centrosome disorganization in fibroblast cultures derived from R6/2 Huntington's disease (HD) transgenic mice and HD patients. Hum Mol Genet 2001; 10(21): 2425-35.

Wang CE, Zhou H, McGuire JR, Cerullo V, Lee B, Li SH*, et al.* Suppression of neuropil aggregates and neurological symptoms by an intracellular antibody implicates the cytoplasmic toxicity of mutant huntingtin. J Cell Biol 2008; 181(5): 803-16.

Supplementary Table 3. One-way ANOVA for qPCR analysis (Fig. 2)

Striatal transcripts	4 weeks	8 weeks
Cnr1	F(3,24) = 10.260, $p < 0.001$	F(3,25) = 52.268, $p < 0.001$
Darpp32	F(3,24) = 3.776, $p = 0.024$	F(3,25) = 65.682, $p < 0.001$
Drd2	F(3,24) = 6.665, $p = 0.002$	F(3,25) = 57.767, $p < 0.001$
Pde10a	F(3,24) = 112.362), $p < 0.001$	F(3,25) = 147.738, $p < 0.001$
Penk1	F(3,24) = 15.791), $p < 0.001$	F(3,25) = 128.157, $p < 0.001$
Cortical transcripts		
BdnfIV	F(3,26) = 3.236, $p = 0.038$	F(3,27) = 11.119, $p < 0.001$
Pgam2	F(3,25, = 4.012, $p = 0.018$	F(3,26) = 27.034, $p < 0.001$
Grm2	F(3,26) = 19.501, $p < 0.001$	F(3,25) = 9.842, $p < 0.001$
Hrh3	F(3,26) = 23.748, $p < 0.001$	F(3,25) = 73.196, $p < 0.001$
Hrt1a	F(3,26) = 6.085, $p = 0.003$	F(3,23) = 55.956, $p < 0.001$
Cerebellar transcripts		
Igfbp5	F(3,26) = 15.483, $p < 0.001$	F(3,25) = 49.670, $p < 0.001$
KcnK2	F(3,27) = 14.233, $p < 0.001$	F(3,25) = 21.277, $p < 0.001$
Nr4a2	F(3,26) = 2.210, $p = 0.111$	F(3,25) = 16.999, $p < 0.001$
Pcp4	F(3,27) = 20.598, $p < 0.001$	F(3,24) = 95.043, $p < 0.001$
Uchl1	F(3,27) = 1.552, $p = 0.224$	F(3,25) = 7.339, $p = 0.001$

Supplementary Table 4. Two-way ANOVA for Seprion-ELISA analysis (Fig. 3A-H)

	2, 4 and 8 weeks of age	8, 16 weeks and end stage
Striatum		
Genotype	F(1,30) = 27.055, $p < 0.001$	F(1,34) = 4.861, $p = 0.034$
Age	F(2,30) = 262.161, $p < 0.001$	F(2,34) = 29.862, $p < 0.001$
Genotype x Age	F(2,30) = 13.972, $p < 0.001$	F(1,34) = 6.974, $p = 0.012$
Cortex		
Genotype	F(1,30) = 47.185, $p < 0.001$	F(1,33) = 0.668, $p < 0.420$
Age	F(2,30) = 146.657, $p < 0.001$	F(2,33) = 36.133, $p < 0.001$
Genotype x Age	F(2,30) = 10.992, $p < 0.001$	F(1,33) = 6.546, $p = 0.0015$
Hippocampus		
Genotype	F(1,30) = 17.636, $p < 0.001$	F(1,34) = 3.203, $p = 0.082$
Age	F(2,30) = 93.781, $p < 0.001$	F(2,34) = 35.686, $p < 0.001$
Genotype x Age	F(2,30) = 5.161, $p = 0.012$	F(1,34) = 16.370, $p < 0.001$
Cerebellum		
Genotype	F(1,29) = 19.696, $p < 0.001$	F(1,34) = 4.250, $p = 0.047$
Age	F(2,29) = 127.696, $p < 0.001$	F(2,34) = 40.299, $p < 0.001$
Genotype x Age	F(2,29) = 8.294, $p = 0.001$	F(1,34) = 0.312, $p = 0.580$

Supplementary Table 5. Statistical analyses for the CAG instability data

One-way ANOVA for CAG repeat instability (Supplementary Fig. 2)

Instability index	
R6/2$(CAG)_{90}$	F(7,111) = 266.7, $p < 0.001$
R6/2$(CAG)_{200}$	F(7,110) = 176.5, $p < 0.001$
Expansion index	
R6/2$(CAG)_{90}$	F(7,111) = 351.8, $p < 0.001$
R6/2$(CAG)_{200}$	F(7,110) = 159.7, $p < 0.001$

Two-way ANOVA for CAG repeat instability (Supplementary Fig. 2)

Instability index	
Tissue	F(7,221) = 356.48, $p < 0.001$
Genotype	F(7,221) = 541.5, $p < 0.001$
Tissue x Genotype	F(7,221) = 34.79, $p < 0.001$
Expansion index	
Tissue	F(7,221) = 340.22, $p < 0.001$
Genotype	F(7,221) = 408.16, $p < 0.001$
Tissue x Genotype	F(7,221) = 38.45, $p < 0.001$

Supplementary Table 6. Two-tailed Student's *t*-test for the nuclear Seprion-ELISA analysis (Fig. 7B)

	4 weeks of age
4C9	t(10) = -6.762, $p < 0.001$
MW8	t(10) = -6.087, $p < 0.001$
	8 weeks of age
4C9	t(9) = 4.771 $p = 0.001$*
MW8	t(9) = 2.829, $p = 0.020$*

*equal variance not assumed

Supplementary Table 7: Two-way ANOVA for FRASE analysis (Fig. 8C)

Genotype	F(3,48) = 184, $p < 0.001$
Age	F(3,48) = 15.3, $p < 0.001$
Genotype x Age	F(9,48) = 13.6, $p < 0.001$

Supplementary Table 8. Statistical analyses for the huntingtin transcript analyses (Supplementary Fig. 3)

Two-tailed Student's *t*-test for *HTT-exon1* transcript at 2 weeks of age (Supplementary Fig. 3A)

Striatum	t(13) = 6.262, $p < 0.001$
Cortex	t(14) = 13.297, $p < 0.001$
Cerebellum	t(14) = 12.549, $p < 0.001$

Two-tailed Student's *t*-test for cortical *HTT-exon1* transcript (Supplementary Fig. 3B)

2 weeks of age	t(13) = 4.031, $p = 0.001$
4 weeks of age	t(12) = 7.184, $p < 0.001$
8 weeks of age	t(13) = 7.439, $p < 0.001$
14 weeks of age	t(11) = 14.610, $p < 0.001$

One-way ANOVA for cortical endogenous *Htt* transcript (Supplementary Fig. 3C)

2 weeks of age	F(3,27) = 0.936, p = 0.437
8 weeks of age	F(3,26) = 0.936, p = 0.493
14 weeks of age	F(3,27) = 2.368, p = 0.093